Available online at www.sciencedirect.com
ScienceDirect
Mathematics and Computers in Simulation 199 (2022) 231–252
MATHEMATICS AND COMPUTERS IN SIMULATION
www.elsevier.com/locate/matcom

Original articles

Robust RRE technique for increasing the order of accuracy of SPH numerical solutions

L.P. da Silva[a,*], C.H. Marchi[b], M. Meneguette[c], A.C. Foltran[d]

[a] *Graduate Program in Numerical Methods in Engineering (PPGMNE), Federal University of Paraná (UFPR), P.O. Box 19011, Zip Code 81531-980, Curitiba, PR, Brazil*
[b] *Laboratory of Numerical Experimentation (LENA), Department of Mechanical Engineering (DEMEC), Federal University of Paraná (UFPR), P.O. Box 19040, Zip Code 81531-980, Curitiba, PR, Brazil*
[c] *São Paulo State University (UNESP), Department of Mathematics and Computer Science (DMC), Zip Code 19060-900, Presidente Prudente, SP, Brazil*
[d] *Graduate Program in Mechanical Engineering (PGMEC), Federal University of Paraná (UFPR), P.O. Box 19040, Zip Code 81531-980, Curitiba, PR, Brazil*

Received 20 May 2021; received in revised form 10 March 2022; accepted 21 March 2022
Available online 28 March 2022

Abstract

This study presents the use of a post-processing technique called repeated Richardson extrapolation (RRE) to improve the accuracy of numerical solutions of local and global variables obtained using the smoothed particle hydrodynamics (SPH) method. The investigation focuses on both the steady and unsteady one-dimensional heat conduction problems with Dirichlet boundary conditions, but this technique is applicable to multidimensional and other mathematical models. By using all the variables of the real type and quadruple precision (extended precision or Real*16) we were able to, for example, reduce the discretization error from *1.67E−08* to *3.46E−33* with four extrapolations, limited only by the round-off error and, consequently, determining benchmark solutions for the variable of interest $\psi(1/2)$ using the SPH method. The increase in CPU time and memory usage owing to post-processing was almost null. RRE has proven to be robust in determining up to a sixteenth order of accuracy in meshless discretization for the spatial domain.

Keywords: SPH with RRE highly accurate scheme; Sixteenth order of accuracy; Heat diffusion; Discretization error; Verification; SPH benchmark solutions

1. Introduction

In computational fluid dynamics (CFD) and computational heat transfer (CHT), there are some numerical methods that do not require domain discretization with a computational mesh. These are meshless methods [2,22,23,41], one of which is smoothed particle hydrodynamics (SPH) [14,26].

* Corresponding author.
E-mail addresses: luciano.silva@ufpr.br (L.P. da Silva), chmcfd@gmail.com (C.H. Marchi), messias.meneguette@unesp.br (M. Meneguette), antoniocarlos.foltran@gmail.com (A.C. Foltran).
URLs: http://lattes.cnpq.br/1873355458944068 (L.P. da Silva), http://www.cfd.ufpr.br/ (C.H. Marchi), http://lattes.cnpq.br/1531018187057108 (M. Meneguette), http://lattes.cnpq.br/0029752439767379 (A.C. Foltran).

https://doi.org/10.1016/j.matcom.2022.03.016

The smoothed particle hydrodynamics (SPH) method has emerged as a promising simulation technique for nonlinear simulations, being able to deal with flows related to complex geometry domains without the need for fine meshes. However, one drawback is its low order.

Despite its adaptability to complex geometries [15,17,34], efforts to overcome the SPH low order are still a field of research. Two ways to improve this are the so-called corrective smoothed particle method (CSPM) [6] and the finite particle method (FPM) [24]. Both techniques increase the number of summation terms for the approximations or append additional terms in the Taylor series to compose the numerical approximation [10,11,13,43]. FPM produces more robust results than CSPM; however, it uses at least six summations and calculates an inverse matrix in each approximation at the position of the particle $\mathbf{x}_i$.

SPH is generally applied to multidimensional mathematical models with complex geometries. However, the low accuracy of the original standard method requires further studies to improve its overall accuracy. Recently, a review of methods to obtain a more accurate SPH approximation has been presented. Techniques or other approaches that alter the standard SPH or consider kernels with higher orders of accuracy are reviewed by Lind et al. [19]. Observing the numerical error of the sixth order of accuracy, which is between *1.0E−13* and *1.0E−15*, we know that it is possible to reduce these magnitudes further without extra computational effort using a technique known as repeated Richardson extrapolation (RRE) [7,28,30–33,42]. The mathematical models chosen in this study are simple to facilitate numerical error analyses, but the technique is robust and can be applied to any mathematical model and any type of geometry [3].

In the literature, it is very common to find the use of Euler's method for time integration when solving mathematical models with SPH [9]. In our work, we choose to solve linear systems of algebraic equations even for problems independent of the time variable. In general, problems involving the time variable are solved explicitly with the SPH method. We solve this implicitly, that is, to determine the numerical solutions, we need to solve the systems of linear equations. In the case of the unsteady heat diffusion equation, we adopted the Crank–Nicolson method, which is unconditionally stable. Thus, the discretization can be refined without the concern of generating impossible systems to solve.

In the present study, we propose a low computational cost technique that may be more efficient than kernel correction techniques [6,24]. By using the standard SPH approximation, we solve the problem over some discretizations, typically from a very coarse to a sufficiently refined one. This was achieved by doubling the number of particles at each new discretization. After solving the problem with SPH for the considered discretizations, we apply the RRE, a post-processing technique that at each level of extrapolation causes the order of accuracy to be increased, achieving very high values, numerical errors with a magnitude on the order of the round-off error, and negligible CPU time and RAM usage. The process only requires that the solutions are situated in the monotonic convergent region (i.e., the number of particles is sufficiently large so that the error is dominated by the first term of the discretization expression and still below the round-off error).

The RRE is a robust technique with low computational cost, which can be applied to any mathematical model, even with higher complexity, such as the Euler equations [20,38,40]. Moreover, its robustness allows it to be applied in cases of structured and unstructured grids [16,28,32]. This flexibility also motivated us to apply RRE to particle discretization. This technique decreases the discretization error and increases the order of accuracy until the computer capacity is reached. For us, this limit is established by the quadruple precision (extended precision or Real*16) that the Fortran 95 language compiler uses. This means that the machine round-off error is in the order of *1.0E−32*. Of course, when the numerical error reaches this order of magnitude in quadruple precision, the round-off error can damage the results.

Similar to methods that use meshes, such as the finite difference method (FDM) and finite volume method (FVM), we believe that it is possible to define coherence tests to evaluate the numerical solutions obtained with the SPH method. These tests allow us to evaluate the consistency and accuracy of the solutions using the variables of interest, which can be primary (midpoint temperature $\Psi(1/2)$) or secondary (average temperature Ψ_{mean}). These coherence tests can complement the already known techniques to improve the approximations obtained with SPH [20,21] and take a step forward in terms of reducing the discretization error, increasing the order of accuracy, and ensuring consistency and convergence of numerical solutions obtained with SPH.

In this study, we consider a method to be consistent if the truncation error of the approximation tends to zero as the number of particles tends to infinity. In this case, the numerical solution tends to the analytical one. Thus, unlike the classic SPH bibliography, consistency for us is no longer measured by the moments of the kernel [24,43]; instead, it is a global tool that evaluates the decrease in the discretization error as a function of the number of particles.

When verifying numerical solutions, we must adopt coherence tests, so that we can identify the sources of numerical errors in numerical solutions. Verification of these numerical solutions requires careful and detailed analysis to prove the veracity of the sources of numerical error [29]. In addition, it is necessary to deepen the knowledge about numerical pollution errors [27]. The definition of this type of error was based on *a posteriori* error estimation [1] and may also be similar to the equation used to show the instability of the round-off error, as in [5, p. 178–179].

The mathematical models selected for this study have characteristics that allow the behavior of the numerical solutions to be evaluated. This is because we choose functions for the source term with the following characteristics: infinitely differentiable functions (C^{∞}), sign change at each new derivative, or constant zero term.

The main goal of our research is to show: (i) an efficient way to decrease the discretization error until the Fortran language compiler reaches the quadruple precision limit; (ii) verify that the RRE is so efficient that the computational time for its execution can be neglected; (iii) combine numerical solutions obtained with different number of particles, always with constant refinement ($q = 2$). By doing so, we intend to achieve: (a) consistent and accurate numerical solutions; (b) sixteenth order of accuracy for numerical solutions of all variables of interest; (c) behavior of the discretization error; and (d) calculation of the orders of accuracy of the numerical solutions (effective orders (p_E) and apparent orders (p_U)). These four items are defined as coherence tests because they can be used to identify numerical errors in numerical solutions calculated using any numerical method.

This paper is structured as follows: In Section 2, we present the mathematical and numerical models used and the variables of interest; in Section 3, we present the methodology used to achieve the goals pointed out in Section 1, Section 4 presents the results for all tests, and Section 5 presents the conclusions.

2. Mathematical and numerical models

The mathematical models chosen for this study are the steady and unsteady 1D heat diffusion equations. We consider three cases with increasing complexity.

In the following sections, the Ψ function represents the analytical solution for the temperature field, ψ the numerical solution, f the source term, and $\mathbf{x} = \mathbf{x}(x)$ or $\mathbf{x} = \mathbf{x}(x, t)$ is the particle position vector which reduces to the coordinate x in one dimension. The subscripts i and j refer to the ith particle and jth neighboring particle, respectively. Ψ_{mean} is the analytical temperature, and ψ_{mean} is the numerical average temperature.

2.1. Mathematical models

The one-dimensional model of steady heat diffusion is

$$\frac{\partial^2 \Psi}{\partial \mathbf{x}^2} = f(\mathbf{x}), \quad 0 \leq \mathbf{x} \leq 1, \tag{1}$$

where $\Psi(0)$ and $\Psi(1)$ are Dirichlet boundary conditions and $\partial^2/\partial \mathbf{x}^2$ is the second derivative with respect to the variable x. The unsteady one-dimensional model of the heat diffusion is

$$\frac{\partial \Psi}{\partial t} = \lambda \frac{\partial^2 \Psi}{\partial \mathbf{x}^2} + f(\mathbf{x}), \quad 0 \leq \mathbf{x} \leq 1, \quad 0 \leq t \leq 1, \tag{2}$$

where $\Psi(0, t)$ and $\Psi(1, t)$ are Dirichlet boundary conditions and λ is the constant thermal diffusivity.

Case I: the source term is an infinitely differentiable function C^{∞} that do not change sign (3).

$$\frac{\partial^2 \Psi}{\partial \mathbf{x}^2} = e^{\mathbf{x}}, \tag{3}$$

with the analytical solution $\Psi(\mathbf{x}) = e^{\mathbf{x}}$ and boundary conditions $\Psi(0) = 1$, $\Psi(1) = e$, and average temperature $\Psi_{mean} = (e - 1)$.

Case II: the source term is an infinitely differentiable function C^{∞} that change sign (4).

$$\frac{\partial^2 \Psi}{\partial \mathbf{x}^2} = -\pi^2 \sin(\pi \mathbf{x}), \tag{4}$$

with the analytical solution $\Psi(\mathbf{x}) = \sin(\pi \mathbf{x})$ and boundary conditions $\Psi(0) = 0$, $\Psi(1) = 0$, and average temperature $\Psi_{mean} = 2/\pi$.

Case III: constant thermal diffusivity λ and zero heat source, according to

$$\frac{\partial \Psi}{\partial t} = \lambda \frac{\partial^2 \Psi}{\partial \mathbf{x}^2}, \tag{5}$$

with the analytical solution $\Psi(\mathbf{x}, t) = \sin(\pi \mathbf{x}) e^{-\pi^2 t}$ when $\lambda = 1$, boundary conditions $\Psi(0, t) = 0$ and $\Psi(1, t) = 0$, and initial condition $\Psi(\mathbf{x}, 0) = \sin(\pi \mathbf{x})$; the average temperature $\Psi_{mean} = (2/\pi) e^{-\pi^2}$ at time $t = 1.0$ s.

2.2. Numerical models

For the results to be obtained correctly, it is important to take some care. Therefore, we define the following discretization characteristics.

Definition 1. A fixed sensor particle $\mathbf{x}_s(\mathbf{Q})$ or $\mathbf{x}_s(\mathbf{Q}, t)$, where $\mathbf{x}_s$ is any chosen particle that has coincident coordinates $\mathbf{Q}$ at all discretization levels and time steps simultaneously.

In all of our cases, the fixed sensor particles $\mathbf{x}_s(\mathbf{Q})$ and $\mathbf{x}_s(\mathbf{Q}, t)$ have coordinates $x = 1/2$ (midpoint) and $t = 1.0\,s$. The expressions $\mathbf{x}_s(x) = 1/2$ or $\mathbf{x}(x_i) = 1/2$ are equivalent. Note that particles with coordinates $x = 1/8, 1/4, 3/4$, and $7/8$ also satisfy Definition 1.

2.2.1. Discretization of the steady heat diffusion equation

We extended the analysis of the local truncation error characteristics (ε_τ) in the FDM and FVM methods [12] to the SPH method [41]. Following this approach, we define the local truncation error [29] as $\mathbf{x}_i$ (particle) as

$$\varepsilon_\tau(\psi) = C_0 \left(kh(\mathbf{x}_i - \mathbf{x}_j)\right)^{p_0} + C_1 \left(kh(\mathbf{x}_i - \mathbf{x}_j)\right)^{p_1} + C_2 \left(kh(\mathbf{x}_i - \mathbf{x}_j)\right)^{p_2} + \cdots + C_n \left(kh(\mathbf{x}_i - \mathbf{x}_j)\right)^{p_n}. \tag{6}$$

The powers $p_0 < p_1 < p_2 < \cdots < p_n$ are the true orders for the non-null terms in the truncation error equation. These true orders are positive integers that usually characterize an arithmetic series as $p_0 \geq 1$, the smallest of which is called asymptotic order. The k scale is used to modify the base radius of the kernel function without the need to change the number of particles in the domain discretization (in practice, we use kh, which is the smoothing length multiplied by the k-factor), in which we choose the simplification effect $h = \Delta x$ (uniform mean particle distance), which is also the smoothing length for $k = 1$. The constant coefficients C_n are independent of h.

The discretization error is generated exclusively by the truncation error

$$\left\langle \frac{\partial^2 \Psi(\mathbf{x}_i)}{\partial \mathbf{x}^2} \right\rangle = \psi(\mathbf{x}_i) + \varepsilon_\tau(\psi(\mathbf{x}_i)). \tag{7}$$

Eq. (8) defines the SPH approximation for the second derivative [4] and its truncation error.

$$\left\langle \frac{\partial^2 \Psi(\mathbf{x}_i)}{\partial \mathbf{x}^2} \right\rangle = 2 \sum_{j \in V_i} \frac{(\psi(\mathbf{x}_i) - \psi(\mathbf{x}_j))}{r_{ij}^2} \frac{m_j}{\rho_j} \mathbf{x}_{ij} . \nabla_i W_{ij} + O(\mathbf{x}_i - \mathbf{x}')^2, \tag{8}$$

$$\frac{\partial^2 \Psi(\mathbf{x}_i)}{\partial \mathbf{x}^2} \approx 2 \sum_{j \in V_i} \frac{(\psi(\mathbf{x}_i) - \psi(\mathbf{x}_j))}{r_{ij}^2} \frac{m_j}{\rho_j} \mathbf{x}_{ij} . \nabla_i W_{ij} \tag{9}$$

and

$$\nabla_i W(\mathbf{x}_{ij}, h) = \frac{\alpha_{w,d} \mathbf{x}_{ij}}{h^{d+1} r_{ij}} \frac{\partial W_{ij}}{\partial \phi}, \tag{10}$$

where m_j and ρ_j are the mass and density of particle $\mathbf{x}_j$, respectively. In addition, $\mathbf{x}_{ij} = \mathbf{x}_i - \mathbf{x}'$, $r_{ij} = \|\mathbf{x}_{ij}\|$, $\alpha_{w,d}$ is a normalization constant, and d is the domain dimension. The kernel gradient $\nabla_i W(\mathbf{x}_{ij}, h)$ is written in terms of the first kernel derivative $\partial W_{ij}/\partial \phi$, as described in *Section* 2.2.4.

From Eq. (8), the discretization of the steady heat diffusion 1D is given by:

$$-\frac{\partial^2 \Psi(\mathbf{x}_i)}{\partial \mathbf{x}^2} = f(\mathbf{x}_i). \tag{11}$$

Since Ψ represents the analytical solution and we consider it to be unknown, we replace Ψ with ψ, which will be the calculated solution, such that

$$-\frac{\partial^2 \psi(\mathbf{x}_i)}{\partial \mathbf{x}^2} = f(\mathbf{x}_i), \tag{12}$$

that is,

$$-2\sum_{j\in V_i} \frac{(\psi(\mathbf{x}_i) - \psi(\mathbf{x}_j))}{r_{ij}^2} \frac{m_j}{\rho_j} \mathbf{x}_{ij}.\nabla_i W_{ij} = f(\mathbf{x}_i). \tag{13}$$

Eq. (13) determines a linear system, where the associated coefficient matrix has principal diagonal elements a_{ii} formed by the sum of all elements a_{ij} of row i for all $j \neq i$ with opposite sign.

2.2.2. Discretization of the unsteady heat diffusion equation

Various forms of temporal integration can be applied in the discretization process. The Crank–Nicolson method was chosen because it has a second-order accuracy $O[h^2, \Delta t^2]$ [23,39]. Thus, we determine approximations for the temporal and spatial derivatives, as observed in Eqs. (14) and (15).

$$\frac{\partial \Psi}{\partial t}(\mathbf{x}_i, t_n) \approx \frac{\psi_i^{n+1} - \psi_i^n}{\Delta t}. \tag{14}$$

$$\frac{\partial^2 \Psi(\mathbf{x}_i, t_n)}{\partial \mathbf{x}^2} \approx 2\sum_{j\in V_i} \frac{(\psi_i^n - \psi_j^n)}{r_{ij}^2} \frac{m_j}{\rho_j} \mathbf{x}_{ij}.\nabla_i W_{ij}. \tag{15}$$

Eq. (2) for $f(\mathbf{x}) = 0$, becomes

$$\frac{\psi_i^{n+1} - \psi_i^n}{\Delta t} = 2\lambda \sum_{j\in V_i} \frac{(\psi_i^n - \psi_j^n)}{r_{ij}^2} \frac{m_j}{\rho_j} \mathbf{x}_{ij}.\nabla_i W_{ij}, \tag{16}$$

which gives the calculated solution.

2.2.3. Crank–Nicolson method for SPH

The Crank–Nicolson method approximates the function $\Psi(\mathbf{x}_i, t_n)$ as the arithmetic mean between the approximations in time n and $n+1$ [5]. Thus, we can approximate the diffusive term to the unsteady heat diffusion equation as follows:

$$\frac{\partial^2 \Psi}{\partial \mathbf{x}^2}(\mathbf{x}_i, t_n) \approx \frac{1}{2}\left[2\sum_{j\in V_i} \frac{m_j}{\rho_j} \frac{(\psi_i^n - \psi_j^n)}{r_{ij}^2} \mathbf{x}_{ij}.\nabla_i W_{ij}\right] + \frac{1}{2}\left[2\sum_{j\in V_i} \frac{m_j}{\rho_j} \frac{(\psi_i^{n+1} - \psi_j^{n+1})}{r_{ij}^2} \mathbf{x}_{ij}.\nabla_i W_{ij}\right]. \tag{17}$$

The temporal derivative shown in Eq. (14) is approximated by the forward Euler method. However, when considering the Crank–Nicolson method for the heat equation, the implicit system of equations (17) takes place. Considering that the compact support (V_i) contains the particles $V_i = \{\mathbf{x}_{i-1},\ \mathbf{x}_{i+1}\}$, or $V_i = \{\mathbf{x}_{i-2}, \mathbf{x}_{i-1}, \mathbf{x}_{i+1}, \mathbf{x}_{i+2}\}$, after some algebraic manipulations, we obtain

$$\sigma\psi_{i-1}^{n+1} + (1-\sigma)\psi_i^{n+1} + \sigma\psi_{i+1}^{n+1} = -\sigma\psi_{i-1}^n + (1+\sigma)\psi_i^n - \sigma\psi_{i+1}^n, \tag{18}$$

where

$$\sigma = \lambda\Delta t\left(\frac{m_j}{\rho_j}\frac{\alpha_{w,d}}{r_{ij}}\frac{\partial W_{ij}}{\partial \phi}\right).$$

Note that the truncation error equation remains the same as defined in Eq. (8), depending only on time.

2.2.4. Kernel SPH

The functions chosen as kernels to be used are the cubic and quartic splines [25,36]

$$W(\phi) = \frac{\alpha_{w,d}}{h^d}\begin{cases} 1 - \frac{3}{2}\phi^2 + \frac{3}{4}\phi^3 & 0 \le \phi < 1 \\ \frac{1}{4}(2-\phi)^3 & 1 \le \phi < 2, \\ 0 & \phi \ge 2 \end{cases} \tag{19}$$

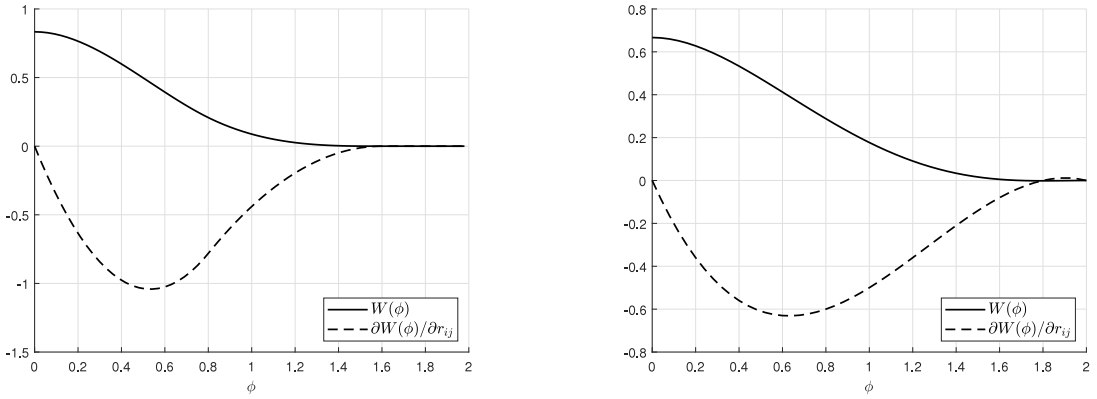

Fig. 1. Generic representation of SPH kernel with first derivative (a) Cubic Spline and (b) Quartic Spline.

with first derivative,

$$\frac{\partial W(\phi)}{\partial r_{ij}} = \frac{\alpha_{w,d}}{h^{d+1}} \begin{cases} -3\phi + \frac{9}{4}\phi^2 & 0 \leq \phi < 1 \\ -\frac{3}{4}(2-\phi)^2 & 1 \leq \phi < 2, \\ 0 & \phi \geq 2 \end{cases} \tag{20}$$

where $\phi = r/h$ and the normalization constant $\alpha_{w,d=1} = 2/3$.

The cubic spline kernel function (19) and its first derivative (20) are shown in Fig. 1(a), while the quartic spline and first derivative, (21) and (22), are shown in Fig. 1(b).

$$W(\phi) = \frac{\alpha_{w,d}}{h^d} \begin{cases} \frac{2}{3} - \frac{9}{8}\phi^2 + \frac{19}{24}\phi^3 - \frac{5}{32}\phi^4 & 0 \leq \phi < 2 \\ 0 & \phi \geq 2 \end{cases}, \tag{21}$$

with first derivative,

$$\frac{\partial W(\phi)}{\partial r_{ij}} = \frac{\alpha_{w,d}}{h^{d+1}} \begin{cases} -\frac{9}{4}\phi + \frac{19}{8}\phi^2 - \frac{5}{8}\phi^3 & 0 \leq \phi < 2 \\ 0 & \phi \geq 2 \end{cases}, \tag{22}$$

where the normalization constant is $\alpha_{w,d=1} = 1$.

3. Methodology

3.1. Verification

The linear system of algebraic equations will be solved using the tridiagonal matrix algorithm (TDMA) solver [5]; therefore, there will be no influence from iteration error. To verify the order of accuracy, we used the effective order (p_E) [29], which shows the asymptotic convergence of the numerical solution based on the error associated with two consecutive discretizations and a constant refinement ratio ($q = h_1/h_2 = 2$) or ($q = h_2/h_3 = 2$), as defined later in Eq. (25). Note that $E((\psi_i)_1)$ refers to the true numerical error (the true numerical error is the difference between the analytical and numerical solutions without using the modulus) in a discretization with few particles (coarse discretization) ($E(\psi_i) = \Psi_i - \psi_i$), and $E((\psi_i)_2)$) is the true numerical error using an immediately more refined discretization ($h_2 = h_1/2$).

The discretization error can be evaluated according to Eq. (23) and by taking two consecutive discretizations as well as its decay, according to Eq. (24) for $q = p = 2$.

$$E(\psi) = C[kh(\mathbf{x}' - \mathbf{x})]^p. \tag{23}$$

$$\frac{E((\psi_i)_1)}{E((\psi_i)_2)} = \frac{C_1[kh_1(\mathbf{x}' - \mathbf{x})]^p}{C_1\,[kh_2(\mathbf{x}' - \mathbf{x})]^p} = \frac{C_1[kh_1(\mathbf{x}' - \mathbf{x})]^p}{C_1\left[\frac{kh_1}{2}(\mathbf{x}' - \mathbf{x})\right]^p} = 2^p = 2^2 = 4, \tag{24}$$

The right hand side (RHS) of Eq. (24) shows that the discretization error is reduced four times at each progressive refinement level with the particles $h_2 = h_1/2$. Note that the $E(\psi_2)/E(\psi_1) = 1/4$ inversion is also true.

By calculating the effective order of the numerical solution with Eq. (25), we find the value of p_E that converges asymptotically to the order of accuracy p, according to

$$p_E = \lim_{h\to 0} \frac{log\left(\frac{|E((\psi_i)_1)|}{|E((\psi_i)_2)|}\right)}{log(q)} \to p, \tag{25}$$

where $q = h_g/h_{g+1} = 2$ is the constant refinement ratio, and g is the reference discretization level. This calculation can also be performed if the analytical solution is unknown. It suffices to consider a linear combination of three solutions with supercoarse (h_1), coarse (h_2), and fine (h_3) discretization, as follows in Eq. (29) [8,29].

In practice, many real cases have no analytical solution; therefore, the error cannot be calculated. An alternative is to estimate the error of the numerical solution (U), defined as [29]:

$$U(\psi) = (\psi_i)_\infty - (\psi_i), \tag{26}$$

where ψ_∞ is the estimated analytical solution defined later in Eq. (30), and the subscript represents the reference particle.

The apparent order (p_U) is defined as the curve of numerical solution error *versus* the uniform distance between the particles (h). In practice, we understand that p_U is an apparent order if $p_U \to p_E \to p$ when $h \to 0$.

The mathematical model of p_U is obtained as follows [8],

$$U(\psi) = K_U h^{p_U}, \tag{27}$$

where K_U is an independent coefficient of h. By substituting Eq. (26) in (27), we obtain

$$\begin{cases} (\psi_i)_\infty - (\psi_i)_{g=1,m} = K_U h_1^{p_U} \\ (\psi_i)_\infty - (\psi_i)_{g=2,m} = K_U h_2^{p_U} \\ (\psi_i)_\infty - (\psi_i)_{g=3,m} = K_U h_3^{p_U} \end{cases}. \tag{28}$$

The unknowns of the system represented by Eq. (28) are ψ_∞, K_U, and p_U. Meanwhile, g is the mesh (number of particle levels) on which the numerical solution was found, and m is the number of extrapolations. For example, $(\psi_i)_1$ represents the variable ψ in the coordinates of particle i at discretization level 1 and at zero extrapolation level ($m = 0$), or equivalently, $(\psi_i)_{g=1,m=0} = (\psi_i)_{1,0}$. For simplicity, we hide subindex m when it is null ($(\psi_i)_1$). Solving this system, we obtain

$$p_U = \frac{log\left(\frac{|(\psi_i)_2 - (\psi_i)_1|}{|(\psi_i)_3 - (\psi_i)_2|}\right)}{log\left(\frac{h_1}{h_2}\right)} \to p, \quad \text{if } h \to 0, \tag{29}$$

$$\psi_\infty = (\psi_i)_3 + \frac{(\psi_i)_3 - (\psi_i)_2}{q^{p_U} - 1}, \quad \text{for } p_U > 0. \tag{30}$$

The value p_U in Eq. (29) represents the average of the local slope of $U(\psi(1/2)_1)$, $U(\psi(1/2)_2)$, $U(\psi(1/2)_3)$, and $(\psi_i)_1, (\psi_i)_2, (\psi_i)_3$ correspond to the variables $\psi(1/2)$ at three consecutive discretization levels. For example, $\psi_1 = \psi(1/2)_1$ (numerical solution at level $N_p = 8$), $\psi_2 = \psi(1/2)_2$ (numerical solution at level $N_p = 16$), and $\psi_3 = \psi(1/2)_3$ (numerical solution at level $N_p = 32$). We consider $E_i = \Psi_i - \psi_i$ the true numerical error.

The average temperature (ψ_{mean}) is calculated by the trapezoidal rule [18]; however, as it is a secondary variable, there is no need to integrate using SPH formalism; thus, we use the classical composite application of the trapezoidal rule as used in the FDM.

$$\psi_{mean} = \frac{h}{2L}\sum_{i=2}^{N_t}(\psi_{i-1} + \psi_i) - \left(\overline{\psi^{ii}}\frac{h^2}{12} + \overline{\psi^{iv}}\frac{h^4}{480} + \overline{\psi^{vi}}\frac{h^6}{53760} + \cdots\right), \tag{31}$$

where $\overline{\psi^{ii}} = \left(\sum_{j=1}^{N_t} \psi_{j-1/2}^{ii}\right) \Big/ N_t$, $\overline{\psi^{iv}} = \left(\sum_{j=1}^{N_t} \psi_{j-1/2}^{iv}\right) \Big/ N_t$, $\overline{\psi^{vi}} = \left(\sum_{j=1}^{N_t} \psi_{j-1/2}^{vi}\right) \Big/ N_t$, where L is the length of the domain, and N_t is the number of nodes in the grid. In addition, N_t denotes the number of particles. The discretization error for the average temperature behaves as shown in Eq. (24), where

$$\frac{E((\psi_{mean})_1)}{E((\psi_{mean})_2)} = \frac{C_1(h_1)^p}{C_1(h_2)^p} = \frac{C_1(h_1)^p}{C_1\left(\frac{h_1}{2}\right)^p} = 2^p = 2^2 = 4. \tag{32}$$

Note that ψ_{mean} is obtained by the trapezoidal rule when integrating using the FDM and the temperature field ψ is obtained with the SPH.

3.2. Repeated Richardson extrapolation

Repeated Richardson extrapolation (RRE) [28,30–33,42] is a post-processing technique that allows to obtain very accurate solutions with a relatively small number of particles, even if low-order schemes are employed.

The RRE has always been applied in simulations with classical methods that use meshes, thus we use it here with the same goal. This is possible because we do not need a mesh to perform the repeated Richardson extrapolation.

The RRE combines solutions of a chosen variable in different meshes, and as extrapolation progresses, discretization errors decrease and the solutions increase in accuracy. The magnitude of such errors obeys true orders (p_m) but can also be based on apparent orders (p_U).

Without any loss, we replace the meshes with several discretizations with particles, as long as they have the same profile, adopting a constant refinement ratio. In this case, it was used as a reference for the SPH discretization model originally of second-order accuracy $p_0 = 2$, with true orders $p_m = \{2, 4, 6, 8, \ldots\}$ deduced *a priori* ($p_0 = \min\{p_m\}$). In fact, when the analytical solution is known, we can calculate p_E, defined *a posteriori*. When the analytical solution is unknown, we can calculate p_U, which is also set *a posteriori*. The elements of the set p_E are the approximations of the elements of the sorted set p_m. In addition, the elements of the set p_U are approximations equivalent to the elements of set p_E, which are also sorted.

Remark: In general there is a standard for the *a priori* deduced true orders. Such a standard can have, for example, increment $\Delta m = 1$ ($p_m = \{2, 3, 4, 5, 6, \ldots\}$) or $\Delta m = 2$ ($p_m = \{2, 4, 6, 8, \ldots\}$) for the second-order accuracy methods. In all the considered cases, the increment is $\Delta m = 2$. These increments are not the only ones that exist and depend on how the numerical schemes were constructed (the increment can be $\Delta m = 3$, we only need to deduce a numerical scheme that considers such information, which is not always easy). What we can state with complete certainty is the fact that if p_E and p_U determine the same orders $p_U = p_E = \{2, 4, 6, 8, \ldots\}$, then $p_m = \{2, 4, 6, 8, \ldots\}$; otherwise, p_E and p_U would not show the same results. Coherence tests, among other things, can confirm this information.

The expression for the RRE is given by equation

$$(\psi_i)_{g,m} = (\psi_i)_{g,m-1} + \frac{(\psi_i)_{g,m-1} - (\psi_i)_{g-1,m-1}}{q^{p_{m-1}} - 1}, \tag{33}$$

where ψ is the numerical solution of the variable of interest on the coordinates of the particle i, g is the mesh (number of particle levels) on which the numerical solution is found, m is the number of extrapolations, p_m are the true orders of the discretization error equation, $q = h_{g-1}/h_g$ is the refinement ratio, and $h = \Delta x = 1/N_{p_i}$. The set $N_{p_i} = \{8, 16, 32, \ldots, 65536\}$ contains the numbers of uniform mean particle spacing (similar to FDM mesh elements).

The theoretical order of accuracy of the numerical solution of ψ, with p_m orders constituting an arithmetic progression and m extrapolations, is

$$p_m = p_0 + m(p_1 - p_0), \tag{34}$$

whereby this equation is valid for $g = [1, G]$, where G is the level with the highest number of particles (most refined level) and $m = [0, g - 1]$.

Mathematically, p_E and p_U are two sets of orders of accuracy that have a number of elements called p_m, that is, $p_E \supset p_m$ and $p_U \supset p_m$. However, the values of p_m for the set p_E are calculated using $|E|$, whereas the values of p_m for the p_U set use only the values of the variable of interest $\psi(1/2)$ or ψ_{mean} obtained with three consecutive discretizations.

Generalizing Eq. (33) for the case in which the apparent orders are applied, we obtain the equations

$$(p_U)_{g,m} = \frac{log\left(\frac{|(\psi_i)_{g-1,m}-(\psi_i)_{g-2,m}|}{|(\psi_i)_{g,m}-(\psi_i)_{g-1,m}|}\right)}{log(q)}, \tag{35}$$

$$(\psi_i)_{g,m} = (\psi_i)_{g,m-1} + \frac{(\psi_i)_{g,m-1} - (\psi_i)_{g-1,m-1}}{q^{(p_U)_{g,m-1}} - 1}. \tag{36}$$

For Eq. (35), the variation between the number of discretizations and extrapolations can be described as $3 \leq g \leq G$ and $0 \leq m \leq$ [integer part $(g-3)/2$]. In Eq. (36), $m = 0$ represents the non-extrapolated solutions $\psi_{g,0}$ (numerical solutions obtained with the SPH). From this, $3 \leq g \leq G$ and $1 \leq m \leq$ [integer part $(g-1)/2$].

We have defined that the $N_p = 8, \ldots, 65536$ set has 14 elements that determine 14 levels of numerical solutions, that is, for $N_p = 8$, we determined a numerical solution level where the domain was discretized with $N_p = 8$ (nine particles). The SPH level is equivalent to a mesh generated with the FDM or FVM. For example, if N_p has 14 elements, then we have 14 solution levels in m_0 to apply the RRE.

In Fig. 2(a), we present the illustration of the RRE to facilitate the understanding of the extrapolations. We need at least three solutions to perform an extrapolation in cases where the analytical solution is unknown. Meanwhile, in Fig. 2(b), we can observe the p_U values associated with each of the extrapolated solutions. Note that the graph is an association of the p_U values, not the nodal value of (ψ_i) at each extrapolation level. The larger the values of g and m, the smaller the discretization error associated with the extrapolated variable. Furthermore, the magnitude of the modulus of the discretization error approaches the magnitude of the round-off error, which can influence the extrapolated numerical solutions. The alternating red and blue colors have no meaning; they are used to enhance the illustration. To apply the RRE $\mathbf{x}_i = \mathbf{x}_s$, that is, $\psi_i = \psi(\mathbf{x}_i) = \psi(\mathbf{x}_s) = \psi(1/2)$, according to Definition 1.

4. Numerical results

The authors implemented a Fortran 95 program that executed the RRE based on numerical solutions obtained with the SPH method. As the purpose of this work is the study of discretization errors and to take advantage of the RRE capability, all real-type variables were declared as quadruple precision. Nonetheless, as a code verification tool, the use of double precision is sufficient. The software used was Microsoft® Visual Studio® 2008 compiler v. 9.0.21022.8 RTM. The hardware architecture has a 3.4 GHz Intel Core (TM)™ i7-6700 processor with 16 GB of RAM hosting 64-bit Windows® 10. The executable file was ran in the GridUNESP cluster.

Consistency is recognized as the mathematical phenomenon that makes the discrete equation match the continuous model (in the limit) as the step size tends to zero (similar to the FDM) [5]. In this study, unlike the SPH literature, we use this definition of consistency as well as replace the step size with the smoothing length. Thus, verification of SPH numerical solutions, as demonstrated in [37], is performed in the three cases proposed in this study to evaluate consistency by decreasing the true numerical error as the number of particles increases. The order of accuracy was evaluated by calculating the effective order (p_E) and apparent order (p_U) for the variables of interest.

Using quadruple precision (Real*16), the numerical solutions with the SPH method were determined using fourteen different levels of discretization for the steady heat diffusion equation (up to 65537 particles) and thirteen for the unsteady heat diffusion equation (up to 32769 particles), varying the number of particles including boundary particles (N_t) $N_t = 9, 17, 33, \ldots, 32769, 65537$ $(N_{p_i} = N_{t_i} - 1)$ and maintaining the constant refinement ratio $q = 2$. For the steady heat diffusion equation, we used $h = \Delta x = 1/N_{p_i}$, and for the unsteady heat diffusion equation, we used the magnitude $\Delta t = \Delta x = h$. The systems have $N_i = N_{t_i} - 2$ unknown, which is equivalent to $N_{t_i} - 2$ particles by excluding the boundary particles. For the unsteady heat diffusion model (case III), the analyses were performed at time $t = 1.0\,s$, i.e., $\psi(1/2, 1)$ and $\psi_{mean}|_{t=1.0\,s}$.

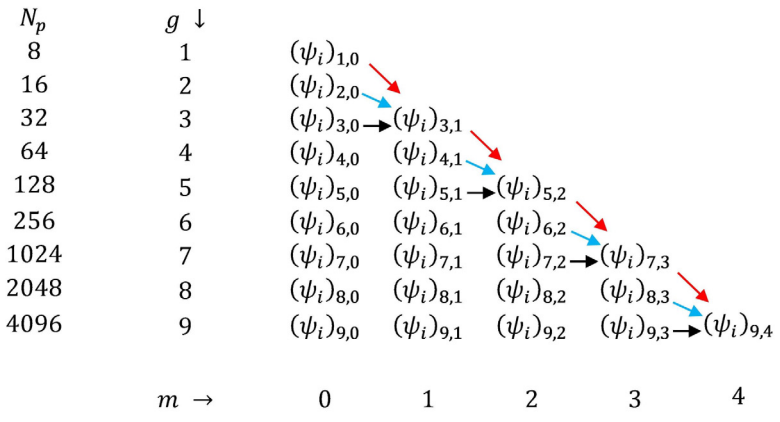

(a)

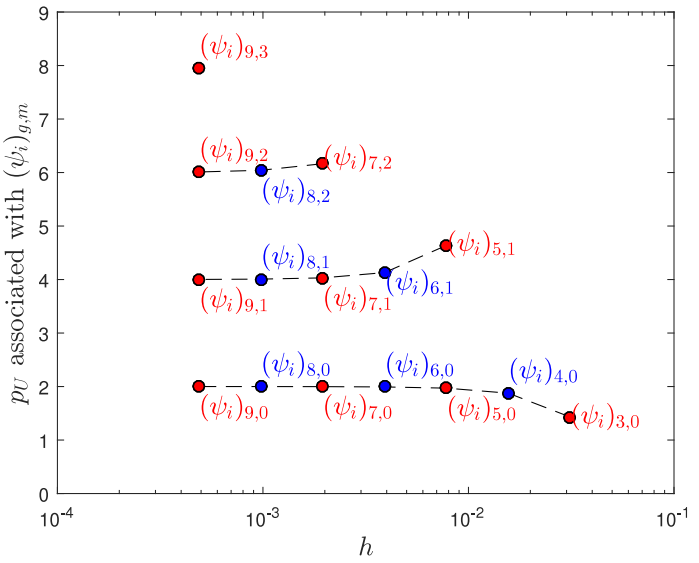

(b)

Fig. 2. (a) Practical scheme for the RRE of numerical solutions and (b) Practical scheme of association of p_U with $(\psi_i)_{g,m}$.

4.1. Verification of numerical solutions for the local variable

The local variable $\psi(1/2)$ was solved using the SPH kernel cubic spline [36] and quartic spline [25], both of which present almost identical results. The correlation between the discretization error and the uniform mean particle distance h is shown in Fig. 3, which displays the classical RRE behavior.

For the first dataset shown in Fig. 3, $m = 0$ represents the discretization error associated with numerical solutions of SPH without extrapolation. The following datasets, $m = 1, 2, \ldots, 7$, show the error associated with the extrapolated solutions obtained with Eq. (33) at successive extrapolation levels. We plotted the results up to $m = 7$, because at this level, the values of the discretization error reach the machine round-off error. Based on these results, we conclude that the discretization error modulus was significantly reduced from *1.67E−08* with *1025* particles to *3.46E−33* with four Richardson extrapolations $m = 4$. The RRE was able to decrease the error magnitude by approximately *24* orders, even when using a relatively small number of particles. The lines $m = 5$, 6, and 7 show that the discretization error is strongly influenced by the machine round-off error. Degeneration (decrease in the

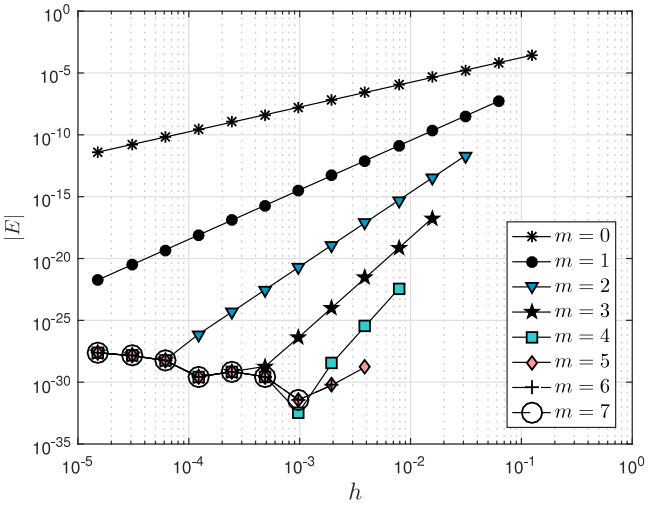

Fig. 3. Discretization errors of temperature at midpoint with RRE for case I with Cubic Spline.

order of accuracy) occurs when the orders of accuracy obtained *a posteriori* are lower than those obtained *a priori*. This numerical effect always appears from left to right in the graphs showing the orders of accuracy (p_U and p_E). Such degenerations indicate that the modulus of the discretization error of a variable of interest has already reached machine precision. This only appears from left to right because the first p_U and p_E values on the right are related to discretizations with few particles. If the discretization considers a small number of particles, it is impossible to reach machine precision, and thus there is no numerical effect of degeneration. We tested several SPH kernels shown in the literature; however, only the cubic and quartic splines determine results that are consistent with our proposal. The other kernel functions we tested require breaking the uniform particle distribution model, and this strategy is not within the scope of this study. Interestingly, both the cubic and quartic splines determine numerically identical results for our models. This is because both kernels determine the same coefficient matrices associated with the systems of linear equations that we are solving. Identical systems produce identical solutions.

Table 1 lists the modulus of the discretization error in each extrapolation. For presentation purposes, the values have two decimal places. However, it is important to understand that the calculations were performed using quadruple precision (Real*16). Note that we use the acronym not applicable (NA) to mark combinations of h and m for which there is no solution. Note that when a new extrapolation is applied, a solution is also lost at the previous level. That is, if we do, for example, five Richardson extrapolations, we will lose the first five solutions obtained in $m = 0$. In the $m = 4$ extrapolation, we have reached the error in the order of *3.46E−33*, which is linked to discretization with *1025* particles. This means that there is no need to continue performing new extrapolations because, from this extrapolation, the discretization error is already influenced by the machine round-off error. Note that the discretization errors linked to h = *6.10E−05* and h = *3.05E−05* are already at a plateau $m = 2$.

In Fig. 4(a), we show the calculation of orders of accuracy using the apparent order (p_U). This means that it is possible to calculate these orders without using the analytical solution. This technique is equivalent to the calculation of the effective order (p_E). We were able to show that it is possible to adopt the two techniques to calculate the orders of accuracy and verify the numerical solutions obtained with the SPH method for the models proposed in this study. Starting at $m = 0$, where $p_0 = 2 \in p_U$, we were able to perform three Richardson extrapolations ($m = 3$) until reaching $p_3 = 8$; in other words, it was possible to determine the order of accuracy equal to 8 for numerical solutions of $\psi(1/2)$. It is important to note that when applying the calculation of p_U, it is necessary to use three consecutive numerical solutions, instead of two, when using p_E. Hence, we are able to obtain results with a higher order of accuracy when using p_E. Note that p_U is a set of orders of accuracy, which can be represented by $p_U = \{p_0, p_1, p_2, p_3, \ldots, p_m\}$, where m represents the number of Richardson extrapolations performed. Generalizing to case I, we have $p_U = \{p_0 = 2, p_1 = 4, p_2 = 6, p_3 = 8\}$, or $p_U = \{2, 4, 6, 8\}$. The negative values that appear in the graph do not exist analytically, because they are purely numerical effects and arise from the discretization error having reached the magnitude of the round-off error (approximately *1.0E−32*).

Table 1
Discretization error modulus with RRE for case I.

h	$m=0$	$m=1$	$m=2$	$m=3$	$m=4$	$m=5$	$m=6$	$m=7$	$m=8$	$m=9$	$m=10$
1.25E−01	*2.73E−04*	NA	NA	NA	NA	NA	NA	NA	NA	NA	NA
6.25E−02	*6.84E−05*	*5.34E−08*	NA	NA	NA	NA	NA	NA	NA	NA	NA
3.12E−02	*1.71E−05*	*3.34E−09*	*2.07E−12*	NA	NA	NA	NA	NA	NA	NA	NA
1.56E−02	*4.28E−06*	*2.09E−10*	*3.23E−14*	*1.77E−17*	NA	NA	NA	NA	NA	NA	NA
7.81E−03	*1.07E−06*	*1.30E−11*	*5.06E−16*	*6.92E−20*	*3.50E−23*	NA	NA	NA	NA	NA	NA
3.90E−03	*2.67E−07*	*8.16E−13*	*7.91E−18*	*2.70E−22*	*3.42E−26*	*1.66E−29*	NA	NA	NA	NA	NA
1.95E−03	*6.68E−08*	*5.10E−14*	*1.23E−19*	*1.05E−24*	*3.40E−29*	*5.81E−31*	*5.77E−31*	NA	NA	NA	NA
9.76E−04	*1.67E−08*	*3.18E−15*	*1.93E−21*	*4.12E−27*	*3.46E−33*	*3.67E−32*	*3.69E−32*	*3.69E−32*	NA	NA	NA
4.88E−04	*4.18E−09*	*1.99E−16*	*3.01E−23*	*1.88E−29*	*2.78E−30*	*2.78E−30*	*2.78E−30*	*2.78E−30*	*2.78E−30*	NA	NA
2.44E−04	*1.04E−09*	*1.24E−17*	*4.71E−25*	*7.09E−30*	*7.04E−30*	*7.05E−30*	*7.05E−30*	*7.05E−30*	*7.05E−30*	*7.05E−30*	NA
1.22E−04	*2.61E−10*	*7.78E−19*	*7.37E−27*	*2.68E−30*	*2.66E−30*	*2.66E−30*	*2.66E−30*	*2.66E−30*	*2.66E−30*	*2.66E−30*	*2.66E−30*
6.10E−05	*6.53E−11*	*4.86E−20*	*5.84E−29*	*5.75E−29*	*5.77E−29*	*5.78E−29*	*5.78E−29*	*5.78E−29*	*5.78E−29*	*5.78E−29*	*5.78E−29*
3.05E−05	*1.63E−11*	*3.04E−21*	*1.36E−28*	*1.40E−28*	*1.40E−28*	*1.40E−28*	*1.40E−28*	*1.40E−28*	*1.40E−28*	*1.40E−28*	*1.40E−28*
1.52E−05	*4.08E−12*	*1.90E−22*	*2.32E−28*	*2.38E−28*	*2.39E−28*	*2.40E−28*	*2.40E−28*	*2.40E−28*	*2.40E−28*	*2.40E−28*	*2.40E−28*

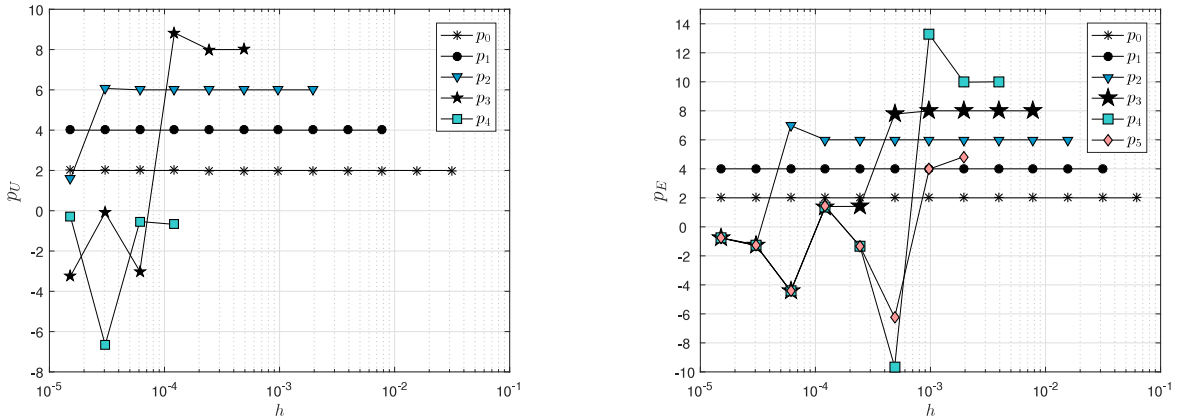

(a) (b)

Fig. 4. (a) Apparent orders (p_U) and (b) effective orders (p_E) of temperature at the midpoint with RRE for case I using the cubic Spline.

This is expected to occur and does not indicate that the numerical solution is diverging. This behavior is called degeneration and means that the extrapolated numerical solutions have the smallest possible discretization error, and it is no longer necessary to extrapolate.

In Fig. 4(b) we show the orders of accuracy using the effective order (p_E). Starting at $m = 0$, where $p_0 = 2 \in p_E$, we were able to perform four Richardson extrapolations ($m = 4$) until reaching $p_4 = 10$; in other words, it was possible to determine the order of accuracy equal to 10 for numerical solutions of $\psi(1/2)$. Note that it was not possible to obtain $p_5 = 12$ in $m = 5$, which means that the calculations were already influenced by the machine round-off error. When this occurs, the values show order degeneration.

The processing time can be considered negligible. Regarding RAM consumption, there is no extra memory usage compared to the explicit method of solving differential equations with SPH. To run the RRE, storage can be considered constant and negligible because we consume only a few kilobytes (KB). In practice, we store the data shown in Table 1 in the computer's memory. For example, the discretization with *8* uniform mean inter-particle distance determines the numerical solution for the temperature field (ψ) and for the average temperature (ψ_{mean}). At each level, we chose two scalar solutions, the temperature at the midpoint $\psi(1/2)$ and the average temperature ψ_{mean}. Using 14 levels, we determine twenty-eight (*14* for each variable) scalar solutions that are used by the RRE. Since these twenty-eight solutions are real numbers, we can consider the CPU time and RAM usage to be constant and negligible. Even if 20 levels of discretization are used, the CPU time and RAM usage are still negligible. For proof, the CPU time to extrapolate all the $\psi(1/2)$ and ψ_{mean} solutions were in the order of *1.99E−02*. In Table 2,

Table 2
CPU time of the solutions of case I.

N_t	h	CPU time (ψ)	CPU time (ψ_{mean})	CPU time (RRE)
9	*1.25E−01*	*2.34E−05*	*2.60E−06*	NA
17	*6.25E−02*	*2.34E−05*	*2.60E−06*	NA
33	*3.12E−02*	*1.95E−05*	*3.90E−06*	1.82E−05
65	*1.56E−02*	*3.90E−05*	*3.90E−06*	2.60E−05
129	*7.81E−03*	*7.41E−05*	*7.80E−06*	3.38E−05
257	*3.90E−03*	*1.20E−04*	*1.56E−05*	5.46E−05
513	*1.95E−03*	*2.26E−04*	*3.90E−05*	6.24E−05
1025	*9.76E−04*	*5.22E−04*	*6.24E−05*	7.28E−05
2049	*4.88E−04*	*1.16E−03*	*7.02E−05*	1.01E−04
4097	*2.44E−04*	*2.78E−03*	*3.14E−04*	1.09E−04
8193	*1.22E−04*	*4.74E−03*	*4.85E−04*	1.17E−04
16385	*6.10E−05*	*8.50E−03*	*1.49E−03*	1.24E−04
32769	*3.05E−05*	*1.55E−02*	*1.99E−03*	3.96E−04
65537	*1.52E−05*	*3.14E−02*	*3.00E−02*	4.61E−04

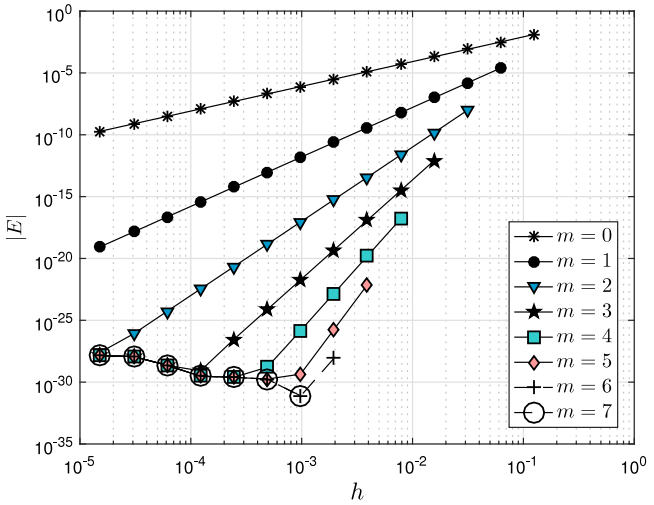

Fig. 5. Discretization errors of temperature at the midpoint with RRE for case II using the cubic Spline.

we show as an example, the CPU time for solving the linear system of algebraic equations in case I. To capture the CPU time from levels *8* to *256*, we averaged the sum of *6000* simulations. From *512* to *8192*, there were *2000*, and from *16384* to *65536*, *20* simulations were sufficient. For the RRE, we averaged *6000* simulations at all levels. This is because the time is so small that it is very difficult to calculate, and the average can ensure greater confidence in the information.

Regarding case II, we can obtain six Richardson extrapolations ($m = 6$), as can be observed in Fig. 5, because at $m = 7$ the discretization error is influenced by the machine round-off error. Next, extrapolations already have a significant influence on the machine round-off error. As a consequence of obtaining $m = 5$, as shown in Fig. 5, we now attain a single result in the order of accuracy equal to 10 for the p_U set, i.e., we find $p_4 = 10 \in p_U$. This can be observed in Fig. 6(a). We understand that the difference between the number of extrapolations in cases I and II is related to the $f(x)$ function that defines the source term in the mathematical model. In case I, we used an exponential function, whereas in case II, the function is trigonometric. This can affect the numerical error by introducing another source of error in addition to the discretization error.

In Fig. 6(b), we show that it was possible to determine the order of accuracy $p_5 = 12 \in p_E$. We note that, at each Richardson extrapolation, we lose a solution (right side of the lines), and the more refined the discretization, the more influential the machine round-off error becomes (lines showing the degeneration of the orders on the left side). It is worth remembering that mathematically, p_E and p_U are two sets of orders of accuracy that have a number

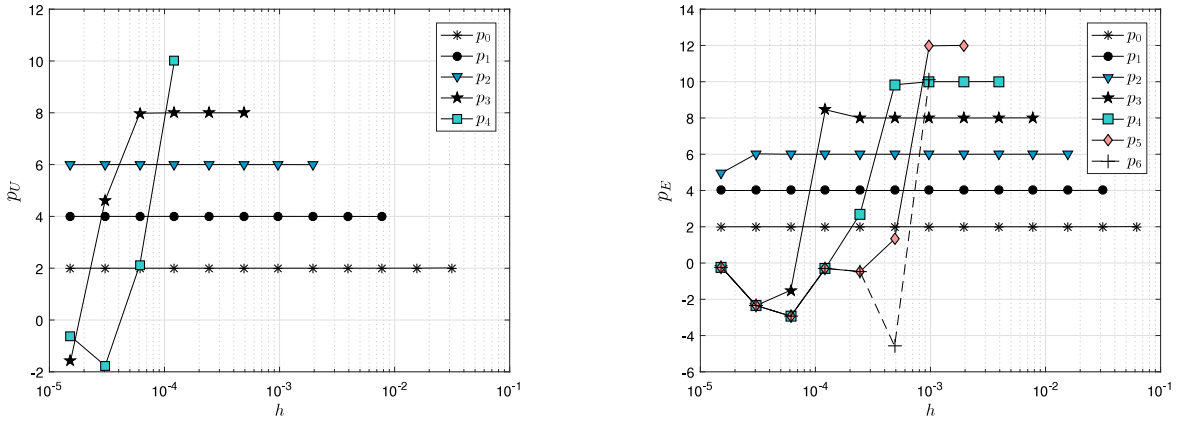

(a) (b)

Fig. 6. (a) Apparent orders (p_U) and (b) effective orders (p_E) of temperature at the midpoint with RRE for case II using the cubic Spline.

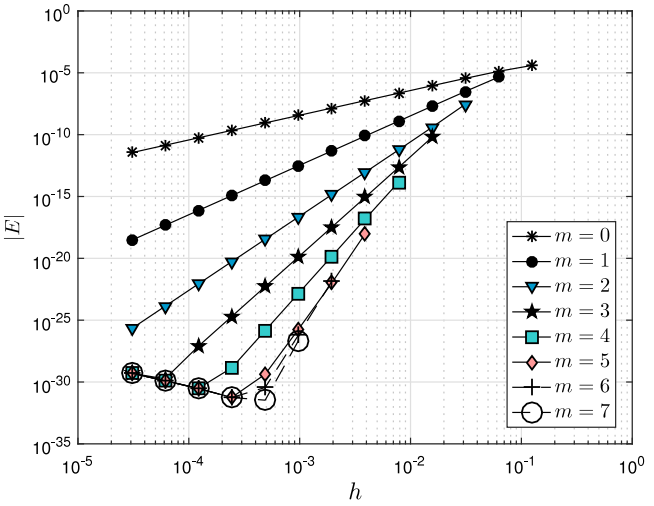

Fig. 7. Discretization errors of temperature at the midpoint with RRE for case III using the cubic Spline.

of elements called p_m, that is, $p_m \subset p_E$ and $p_m \subset p_U$. However, the values of p_m for the p_E set were calculated using $|E|$, whereas the values of p_m for the p_U set use only the values of the variable of interest $\psi(1/2)$ or ψ_{mean} obtained with three consecutive discretizations.

Next, we analyze the results obtained for the mathematical model of unsteady heat diffusion. In Fig. 7, we can observe that the error modulus decreases more slowly than in cases of steady diffusion. However, we were able to determine even more accurate solutions.

Note in Fig. 8(a), we were able to determine numerical solutions with the order of accuracy $p_3 = 8$, because in p_4, the solutions are already influenced by the round-off error.

By analyzing the effective orders found for the problem proposed in case III, we were able to significantly reduce the modulus of the discretization error in such a way that it was possible to determine a numerical solution with the order of accuracy $p_7 = 16$ with seven Richardson extrapolation ($m = 7$) for the primary variable $\psi(1/2)$ with the SPH kernel, as shown in Fig. 8(b). In terms of the discretization error modulus, it was possible to attain, for $m = 0$, the value of *8.87E−10* with *2049* particles up to $m = 7$, with a value of *3.39E−32*, associated to discretization with *2049* particles, thus reducing approximately *22* orders of magnitude. In this case (III), we used *13* discretizations, always with $q = 2$ and varying from $N_p = 8$ to $N_p = 32768$. Based on the results, we realized that it would not be necessary to use discretizations for $N_t > 2049$ particles, because they are associated with solutions that were

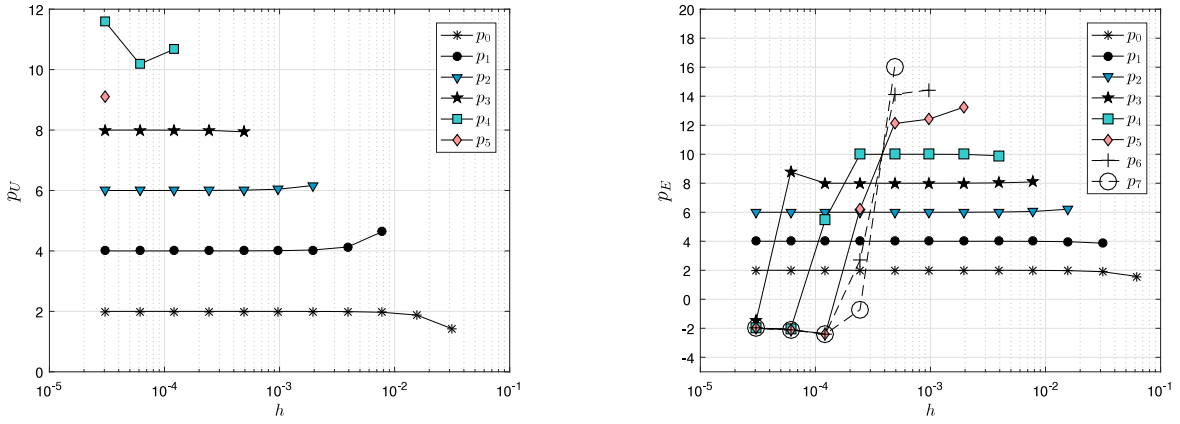

Fig. 8. (a) Apparent orders (p_U) and (b) effective orders (p_E) of temperature at the midpoint with RRE for case III using the cubic Spline.

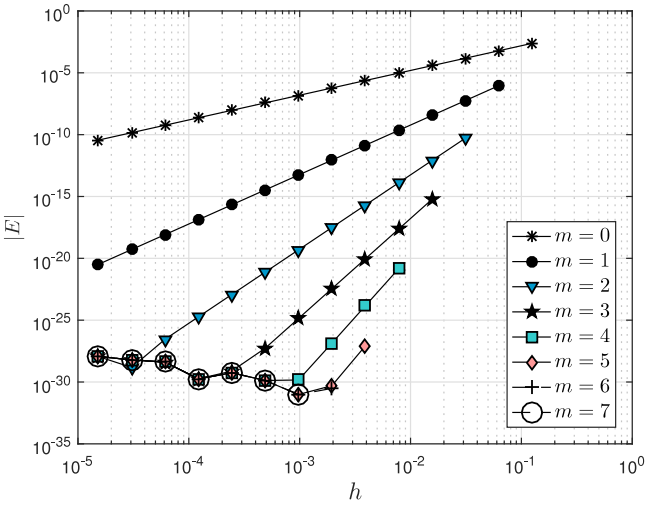

Fig. 9. Discretization errors of average temperature with RRE for case I using the cubic Spline.

extrapolated with the RRE and because they influence the machine round-off error. All results presented for the primary variable $\psi(1/2)$ were numerically identical to those of the two SPH kernels adopted in the approximations.

4.2. Verification of numerical solutions for the global variable

In this section, we verify the numerical solutions for the secondary variable ψ_{mean}, known as the global variable, determined from the numerical model presented in Eq. (31). Note in Fig. 9 for case I, for $m = 6$ the modulus of the average temperature discretization error is already influenced by the machine round-off error. This means that it is unnecessary to continue applying Richardson extrapolations, since the method has reached the machine precision limit for variables of the real type in the program.

We were able to determine the order of accuracy $p_3 = 8$ for ψ_{mean} in $m = 3$ using p_U. Note in Fig. 10(a), in $m = 4$, the value of p_4 is completely degenerated (the order of accuracy obtained a posteriori is lower than that deduced a priori, because the values are completely polluted by the round-off error.) In these cases, the order of accuracy shows degeneration because the modulus of the discretization error value associated with a given h reached its lowest possible value and increased again in the immediately more refined discretization.

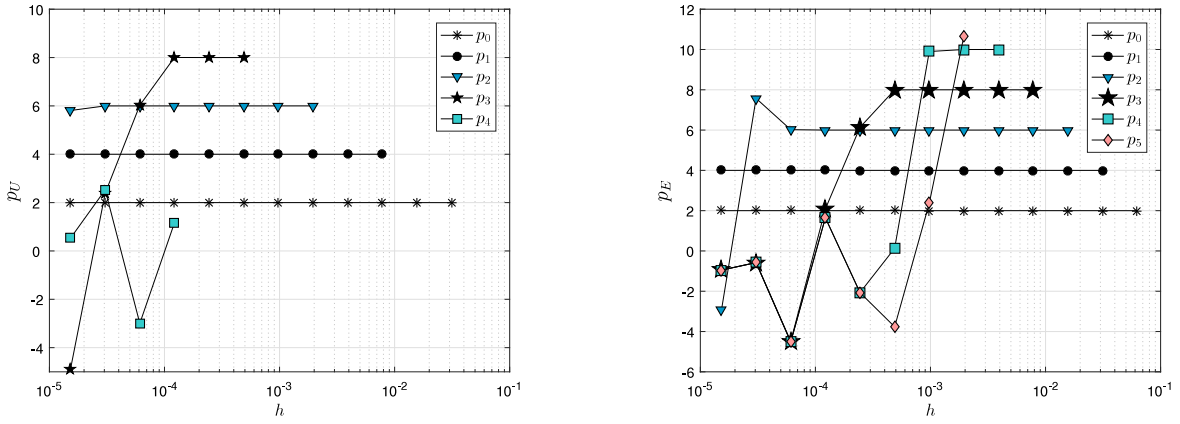

(a) (b)

Fig. 10. (a) Apparent orders (p_U) and (b) effective orders (p_E) of average temperature with RRE for case I using the cubic Spline.

Note in Fig. 10(b), it was possible to determine an order of accuracy equal to 10 for ψ_{mean} by calculating p_E ($p_4 = 10$ in $m = 4$). For $m = 5$, the results are already influenced by the machine round-off error.

When observing the behavior of the discretization error modulus for variable ψ_{mean} in Fig. 11 (case II), we notice that the lines $m = 0$ and $m = 1$ are parallel, this shows that the order of accuracy of the numerical solutions without applying the RRE ($m = 0$) and when applying a single Richardson extrapolation ($m = 1$) behave in the same way but the error increases. To understand the mathematical phenomenon that caused this change in the expected results, it is necessary to develop expertise in what we understand to be recognized as a numerical pollution error (ε_{np}) based on [5,29]. To facilitate this understanding, in Eqs. (37)–(40), we introduce the numerical schemes with their respective terms of numerical pollution error and truncation error for the variables of primary and secondary interest, respectively:

$$\nabla^2 \Psi(\mathbf{x}_i) = 2 \sum_{j \in V_i} \frac{(\psi(\mathbf{x}_i) - \psi(\mathbf{x}_j))}{r_{ij}^2} \frac{m_j}{\rho_j} \mathbf{x}_{ij} . \nabla_i W_{ij} + \varepsilon_{np}(\psi(\mathbf{x}_i)) + \varepsilon_\tau(\psi(\mathbf{x}_i)), \tag{37}$$

where

$$\varepsilon_{np}(\psi(\mathbf{x}_i)) = 2 \sum_{j \in V_i} \frac{(E(\psi(\mathbf{x}_i)) - E(\psi(\mathbf{x}_j)))}{r_{ij}^2} \frac{m_j}{\rho_j} \mathbf{x}_{ij} . \nabla_i W_{ij}, \tag{38}$$

and

$$\Psi_{mean} = \frac{h}{2L} \sum_{i=2}^{N} (\psi_{i-1} + \psi_i) + \varepsilon_{np}(\psi_{mean}) + \varepsilon_\tau(\psi_{mean}), \tag{39}$$

in which

$$\varepsilon_{np}(\psi_{mean}) = \frac{h}{2L} \sum_{i=2}^{N} (E(\psi_{i-1}) + E(\psi_i)). \tag{40}$$

As we know the analytical solution to this problem, the numerical pollution error can be calculated and added to the numerical solution of the variables of interest. The sum $\psi_{mean} + \varepsilon_{np}(\psi_{mean})$ completely corrects the numerical solutions that present an unexpected error profile. We carry out this procedure only to investigate the source of the numerical error that changed the expected results for the variable of interest ψ_{mean} in $m = 0$. It is important to highlight that the numerical pollution error can appear in any numerical scheme (see Eqs. (37)–(40)), but in general, its effects are negligible. In our example, we notice the predominance of the numerical pollution error (initially unknown), owing to our methodology of verification of numerical solutions using coherence tests (analysis of graphs of $|E|$, p_U, and p_E). The corrected results are not shown, as it is common for us to solve problems where the analytical solution is unknown. In such cases, it can be difficult to calculate the numerical pollution error, since

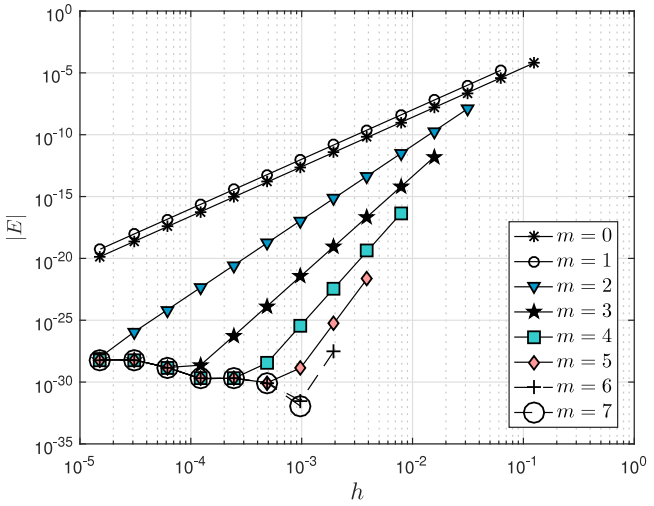

Fig. 11. Discretization errors of average temperature with RRE for case II using the cubic Spline.

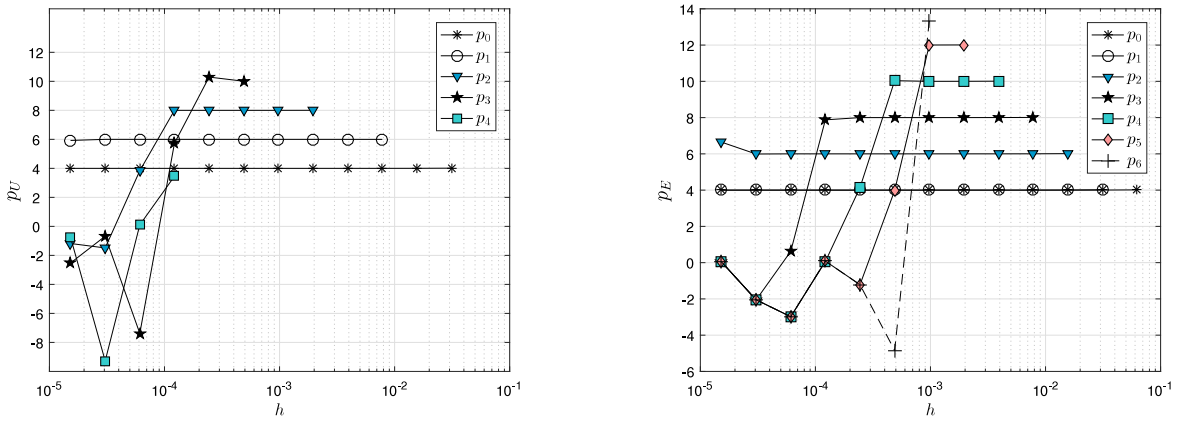

(a) (b)

Fig. 12. (a) Apparent orders (p_U) and (b) effective orders (p_E) of average temperature with RRE for case II using the cubic Spline.

we need to determine an estimated analytical solution for this purpose. Since we know how the numerical pollution error behaves, we can state that $\varepsilon_{np}(\psi_{mean})$ is responsible for the unexpected change in the numerical solution profile ψ_{mean} in $m = 0$, shown in Fig. 11 for the discretization error modulus, in Fig. 12(a) for the apparent order (p_U), and in Fig. 12(b) for the effective order (p_E). We were careful to reproduce the numerical tests using the FDM and were able, through the coherence tests, to obtain the same behavior as the numerical solutions with the SPH method. The coupling (ψ_{mean} + $\varepsilon_{np}(\psi_{mean})$) using the FDM also corrected the profile of the solutions ψ_{mean} in $m = 0$.

In Table 3, we can observe the comparison between the true orders (p_m) of accuracy deducted *a priori* and the apparent (p_U) and effective (p_E) orders of accuracy calculated *a posteriori*. It is easy to notice that the RRE corrected the failure that generated an overestimated order of accuracy for p_E ($p_0 = 4$). We notice that from p_1, the values coincide with the p_m values at all levels. This behavior was not repeated with p_U, where the values remained overestimated.

In Fig. 13 (case III), we can see that it was possible to apply the RRE up to $m = 7$, where the magnitude of the discretization error reached the magnitude of the round-off error. Note that at $m = 7$, we determine two solutions that are not influenced by the round-off error. These solutions are associated with $N_t = 1025$ and $N_t = 2049$ particles. The results show that there is no need to solve the numerical model using many different values for N_t.

Table 3
Comparison of the orders of accuracy of the variable ψ_{mean} of case II.

m	p_m (*a priori*)	p_U (*a posteriori*)	p_E (*a posteriori*)
0	$p_0 = 2$	$p_0 = 4$	$p_0 = 4$
1	$p_1 = 4$	$p_1 = 6$	$p_1 = 4$
2	$p_2 = 6$	$p_2 = 8$	$p_2 = 6$
3	$p_3 = 8$	$p_3 = 10$	$p_3 = 8$
4	$p_4 = 10$	NA	$p_4 = 10$
5	$p_5 = 12$	NA	$p_5 = 12$

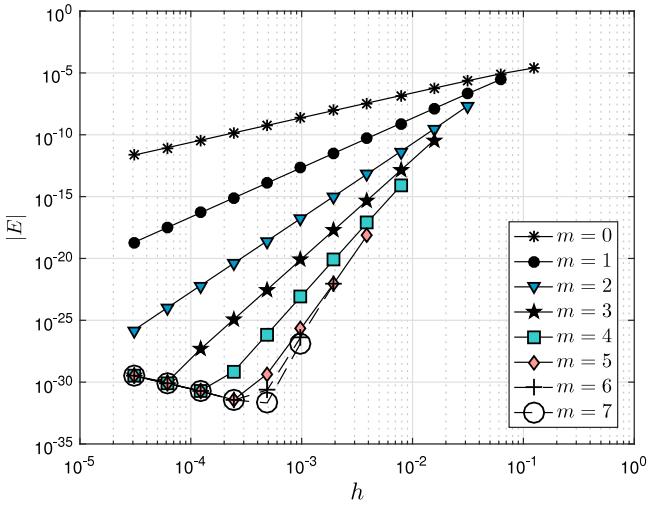

Fig. 13. Discretization errors of average temperature with RRE for case III using the cubic Spline.

By using $N_t = 2049$ particles to fill the domain, we achieve the maximum number of extrapolations necessary for $m = 7$; thus, the discretization error is not influenced completely by the round-off error. Solving systems for $N_i \geq 4095$ particles would be an unnecessary computational effort.

The results of Fig. 14(a) show that it was possible to attain solutions at the order of accuracy equal to 8 using p_U. Note that p_4 does not exhibit asymptotic behavior, thus we believe that in this case, the highest order of accuracy obtained was 8.

Figs. 14(a) and 14(b) clearly show the differences between the p_U and p_E orders obtained. The apparent order did not show the same degeneration as the effective order. This may be due to the effects of the temporal derivative, which as we know, converges more slowly than the spatial derivative. We also noticed that p_E reached the magnitude of the round-off error at the order of accuracy equal to 16, and in general, this occurs when the order is equal to 10.

In Fig. 15 (case III), we show a comparison between the true orders deducted *a priori* (p_m) and the effective orders (p_E) of the variables of interest $\psi(1/2)$ and ψ_{mean} determined a *a posteriori*. The orders shown are the highest obtained in each of the extrapolations until reaching the order of accuracy equal to 16, which was the best result obtained among the three cases. In practice, we selected the most accurate numerical solution for the variables of interest in each extrapolation and associated it with its corresponding h value. This was done to highlight that it is not necessary to use a very small h to determine numerical solutions with high order of accuracy. We choose p_E because it is the most precise method, as it is possible to calculate the modulus of the true numerical error. It is important to note that p_m is an infinite set, as it is an analytical method for determining the order of accuracy. On the other hand, both p_E and p_U are finite sets of orders of accuracy, as they are obtained numerically and within the asymptotic convergence region.

In Table 4, we summarize the variables of interest and the orders of accuracy obtained *a priori* and *a posteriori* for each of the three cases presented in this study. Note that the primary variable $\psi(1/2)$ was obtained using the SPH

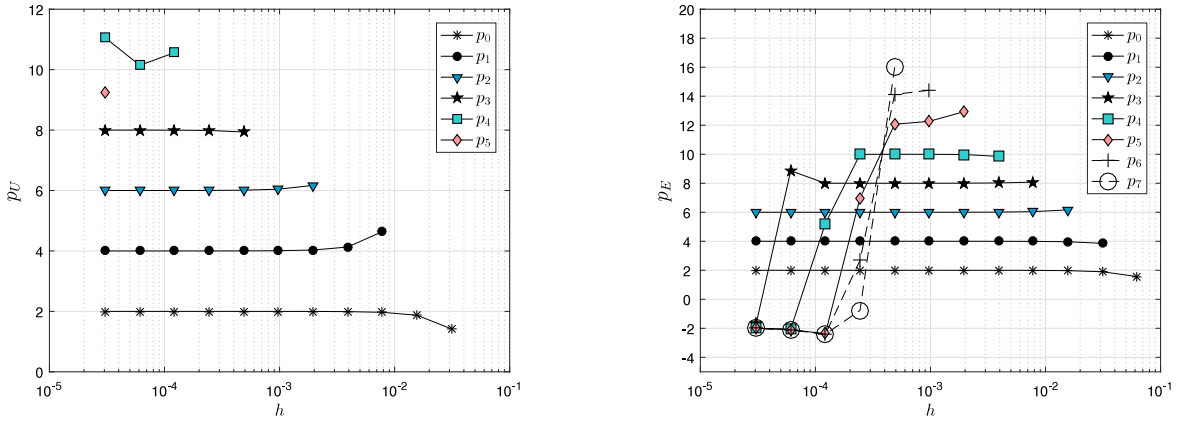

(a) (b)

Fig. 14. (a) Apparent orders (p_U) and (b) effective orders (p_E) of average temperature with RRE for case III using the cubic Spline.

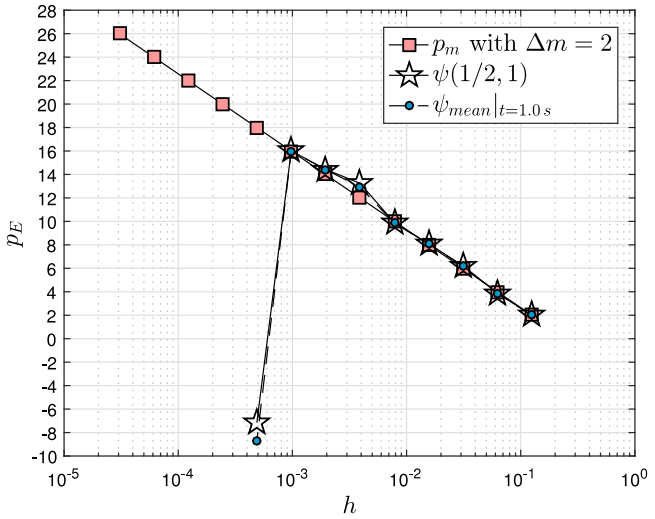

Fig. 15. Effective orders (p_E) of temperature at the midpoint and average temperature with RRE of case III using the cubic Spline.

method and the secondary variable ψ_{mean} with the trapezoidal rule. Both methods have a second-order accuracy at $m = 0$. The two variables of interest in all three cases shown here determine the same orders of accuracy at all levels, except for variable ψ_{mean} in case II, which had a profile change due to the characteristics of the function defined in the source term. This may have caused instability in the round-off error due to the contribution of the derivatives. The orders obtained for $\psi(1/2)$ and ψ_{mean} may indicate that we achieved the same results profile with the SPH method as when using the FDM and FVM.

In Table 5, we show the benchmark SPH solutions for the three detailed cases. Because we solved the average temperature (ψ_{mean}) with the FDM, we realize that it is not appropriate to claim that we have produced reference solutions for this variable of interest. We note that with SPH and RRE, we were able to reduce the discretization error even more than the results shown in [35] when solving the same unsteady heat diffusion equation using the FDM.

5. Conclusions

We demonstrated how to apply the RRE to SPH solutions to decrease the discretization error. We calculated the numerical solutions by varying the number of particles from $N_t = 9, \ldots, 65537$ for the steady heat diffusion

Table 4
Summary of orders of accuracy found *a priori* and *a posteriori*.

Cases	Variables	p_m (*a priori*)	p_U (*a posteriori*)	p_E (*a posteriori*)	Figures
Case I	$\psi(1/2)$	{2, 4, 6, 8, ...}	{2, 4, 6, 8}	{2, 4, 6, 8, 10}	4(a), 4(b)
Case II	$\psi(1/2)$	{2, 4, 6, 8, ...}	{2, 4, 6, 8, 10}	{2, 4, 6, 8, 10, 12}	6(a), 6(b)
Case III	$\psi(1/2)$	{2, 4, 6, 8, ...}	{2, 4, 6, 8}	{2, 4, 6, 8, 10, 12, 14, 16}	8(a), 8(b)
Case I	ψ_{mean}	{2, 4, 6, 8, ...}	{2, 4, 6, 8}	{2, 4, 6, 8, 10}	10(a), 10(b)
Case II	ψ_{mean}	{2, 4, 6, 8, ...}	{4, 6, 8, 10}	{4, 4, 6, 8, 10, 12}	12(a), 12(b)
Case III	ψ_{mean}	{2, 4, 6, 8, ...}	{2, 4, 6, 8}	{2, 4, 6, 8, 10, 12, 14, 16}	14(a), 14(b)

Table 5
SPH benchmark solutions for $\psi(1/2)$.

Case	Analytical solution	Numerical solution	True numerical error
I	*1.64872127070012814684865078781416E+00*	*1.64872127070012814684865078781416E+00*	*3.46667389989702453550076029665286E−33*
II	*1.00000000000000000000000000000000E+00*	*9.99999999999999999999999999999926E−01*	*7.35705238755924095867383574067442E−32*
III	*5.17231862038123061454650903823937E−05*	*5.17231862038123061454650903484924E−05*	*3.39012100579407388383180429840280E−32*

model and $N_t = 9, \ldots, 32769$ for the unsteady heat diffusion model. With this, we realize that it is possible to decrease the discretization error until the magnitude of the machine round-off error is reached. Furthermore, it is not necessary to calculate highly refined solutions to achieve the optimum solution. We used 13 and 14 levels of discretization for particles, with a constant refinement ratio $q = 2$ for the steady and unsteady heat diffusion models, respectively. With this, we verified that only nine levels of discretization are sufficient to reach the optimal solution with a discretization error magnitude of approximately *1.0E−32* and an order of accuracy equal to 12 for the steady heat diffusion model. We also determined the optimal solution for the unsteady heat diffusion model with a discretization error magnitude of approximately *1.0E−32* and an order of accuracy equal to 16.

Other noteworthy results were:

1. We showed how to perform verification of the numerical solutions obtained with SPH by means of coherence tests;
2. We showed the deduction of the numerical pollution error and its effects on the solutions obtained with the SPH method;
3. We defined the discretization scheme with a fixed sensor particle;
4. We showed SPH numerical solutions obtained with implicit and unconditionally stable methods for the unsteady heat diffusion model;
5. We have greatly increased the order of accuracy without increasing CPU time with negligible use of RAM; and
6. We determined benchmark solutions for the variable of interest $\psi(1/2)$ with the SPH method and RRE.

Acknowledgments

The authors would like to thank the Brazilian Space Agency (AEB), National Council of Technological and Scientific Development (CNPq, Brazil), and the Graduate Program of Numerical Methods in Engineering (PPGMNE) from the Federal University of Paraná, Curitiba, PR, Brazil. This study was supported by the resources supplied by the Center for Scientific Computing (NCC/GridUNESP) of São Paulo State University (UNESP) and the support of the Laboratory of Numerical Experimentation (LENA). The second author was supported by a CNPq scholarship. The authors would also like to acknowledge the referees suggestions. This study was financed in part by the Coordenação de Aperfeiçoamento de Pessoal de Nível Superior - Brasil (CAPES) - Finance Code 001.

References

[1] I. Babuška, F. Ihlenburg, T. Strouboulis, S.K. Gangaraj, A *posteriori* error estimation for finite element solutions of Helmholtz' equation. Part I: The quality of local indicators and estimators, Internat. J. Numer. Methods Engrg. 40 (18) (1997) 3443–3462.

[2] T. Belytschko, Y. Krongauz, D. Organ, M. Fleming, P. Krysl, Meshless methods: an overview and recent developments, Comput. Methods Appl. Mech. Engrg. 139 (1996) 3–47.

[3] G. Bertoldo, C.H. Marchi, Verification and validation of the foredrag coefficient for supersonic and hypersonic flow of air over a cone of fineness ratio 3, Appl. Math. Model. 44 (2017) 409–424.

[4] L. Brookshaw, A method of calculating radiative heat diffusion in particle simulations, Proc. Astron. Soc. Aust. 6 (1985) 207–210.
[5] R.L. Burden, J.D. Faires, A.M. Burden, Numerical Analysis, tenth ed., 2016,
[6] J.K. Chen, J.E. Beraun, T.C. Carney, A corrective smoothed particle method for boundary value problems in heat conduction, Internat. J. Numer. Methods Engrg. 46 (1999) 231–252.
[7] L.P. da Silva, B.B. Rutyna, A.R.S. Righi, M.A.V. Pinto, High order of accuracy for Poisson equation obtained by grouping of repeated Richardson extrapolation with fourth order schemes, CMES Comput. Model. Eng. Sci. 128 (2) (2021) 699–715.
[8] G. de Vahl Davis, Natural convection of air in a square cavity: a bench mark numerical solution, Internat. J. Numer. Methods Fluids 3 (3) (1983) 249–264.
[9] J.M. Domínguez, G. Fourtakas, C. Altomare, R.B. Canelas, A. Tafuni, O. García-Feal, I. Martínez-Estévez, A. Mokos, R. Vacondio, A.J.C. Crespo, et al., DualSPHysics: from fluid dynamics to multiphysics problems, Comput. Part. Mech. (2021).
[10] R. Fatehi, M. Fayazbakhsh, M. Manzari, On discretization of second-order derivatives in smoothed particle hydrodynamics, in: Proceedings of World Academy of Science, Engineering and Technology, vol. 30, Citeseer, 2008, pp. 243–246.
[11] R. Fatehi, M.T. Manzari, Error estimation in smoothed particle hydrodynamics and a new scheme for second derivatives, Comput. Math. Appl. 61 (1) (2011) 482–498.
[12] J.H. Ferziger, M. Perić, Computational Methods for Fluid Dynamics, Springer Science & Business Media, 2012.
[13] E. Francomano, M. Paliaga, Highlighting numerical insights of an efficient SPH method, Appl. Math. Comput. 339 (2018) 899–915.
[14] V. Gingold, J.J. Monaghan, Smoothed particle hydrodynamics - theory and application to non-spherical stars, R. Astron. Soc. 181 (1977) 375–389.
[15] Z. Ji, M. Stanic, E.A. Hartono, V. Chernoray, Numerical simulations of oil flow inside a gearbox by Smoothed Particle Hydrodynamics (SPH) method, Tribol. Int. 127 (2018) 47–58.
[16] F. Juretić, A.D. Gosman, Error analysis of the finite-volume method with respect to mesh type, Numer. Heat Transfer B 57 (6) (2010) 414–439.
[17] P.K. Koukouvinis, J.S. Anagnostopoulos, D.E. Papantonis, SPH method used for flow predictions at a turgo impluse turbine: comparison with fluent, World Acad. Sci. Eng. Tecnol. 55 (2011).
[18] E. Kreyszig, Advanced Engineering Mathematics, first ed., John Wiley & Sons, 1999.
[19] S.J. Lind, B.D. Rogers, P.K. Stansby, Review of smoothed particle hydrodynamics: towards converged Lagrangian flow modelling, Proc. R. Soc. Lond. Ser. A Math. Phys. Eng. Sci. 476 (2241) (2020) 20190801.
[20] S.J. Lind, P.K. Stansby, High-order Eulerian incompressible Smoothed Particle Hydrodynamics with transition to Lagrangian free-surface motion, J. Comput. Phys. 326 (2016) 290–311.
[21] S. Litvinov, X.Y. Hu, N.A. Adams, Towards consistence and convergence of conservative SPH approximations, J. Comput. Phys. 301 (2015) 394–401.
[22] G.R. Liu, Mesh Free Methods: Moving beyond the Finite Element Method, CRC Press, 2002.
[23] G.R. Liu, M.B. Liu, Smoothed Particle Hydrodynamics: A Meshfree Particle Method, first ed., World Scientific Publishing, 2003.
[24] M.B. Liu, G.R. Liu, Restoring particle consistency in smoothed particle hydrodynamics, Appl. Numer. Math. 56 (2006) 19–36.
[25] M.B. Liu, G.R. Liu, K. Lam, Construing smoothed functions in smoothed particle hydrodynamics with applications, J. Comput. Appl. Math. 155 (2003) 263–284.
[26] L.B. Lucy, A numerical approach to the testing of the fission hypothesis, Astron. J. 82 (1977) 1013–1024.
[27] C.H. Marchi, Verification of Unidimensional Numerical Solutions in Fluid Dynamics (Ph.D. thesis), Federal University of Santa Catarina, Florianópolis, Brazil, 2001 (in Portuguese).
[28] C.H. Marchi, L.K. Araki, A.C. Alves, R. Suero, S.F.T. Gonçalves, M.A.V. Pinto, Repeated Richardson extrapolation applied to the two-dimensional Laplace equation using triangular and square grids, Appl. Math. Model. 37 (2013) 4661–4675.
[29] C.H. Marchi, A.F.C. da Silva, Unidimensional numerical solution error estimation for convergent apparent order, Numer. Heat Transfer B 42 (2) (2002) 167–188.
[30] C.H. Marchi, E.M. Germer, Effect of the CFD numerical schemes on Repeated Richardson Extrapolation (RRE), Appl. Comput. Math. 2 (2013) 128.
[31] C.H. Marchi, F.F. Giacomini, C.D. Santiago, Repeated Richardson extrapolation to reduce the field discretization error in comptational fluid dynamics, Numer. Heat Transfer B 70 (4) (2016) 340–353.
[32] C.H. Marchi, M.A. Martins, L.A. Novak, L.K. Araki, M.A.V. Pinto, S.F.T. Gonçalves, D.F. Moro, I.S. Freitas, Polynomial interpolation with repeated Richardson extrapolation to reduce discretization error in CFD, Appl. Math. Model. 40 (21–22) (2016) 8872–8885.
[33] C.H. Marchi, L.A. Novak, C.D. Santiago, A.P.S. Vargas, Highly accurate numerical solutions with repeated Richardson extrapolation for 2D Laplace equation, Appl. Math. Model. 37 (2013) 7386–7397.
[34] J.C. Marongiu, F. Leboeuf, E. Parkinson, Numerical simulation of the flow in a Pelton turbine using the meshless method smoothed particle hydrodynamics: a new simple solid boundary treatment, Proc. Inst. Mech. Eng. A 221 (2007).
[35] F.E. Merga, H.M. Chemeda, Modified Crank–Nicolson scheme with Richardson extrapolation for one-dimensional heat equation, Iran. J. Sci. Technol. Trans. A Sci. (2021) 1–10.
[36] J.J. Monaghan, J.C. Lattanzio, A refined particle method for astrophysical problems, Astron. Astrophys. 149 (1985) 135–143.
[37] W.L. Oberkampf, T.G. Trucano, Verification and validation in computational fluid dynamics, Prog. Aerosp. Sci. 38 (3) (2002) 209–272.
[38] G. Oger, M. Doring, B. Alessandrini, P. Ferrant, An improved SPH method: Towards higher order convergence, J. Comput. Phys. 225 (2) (2007) 1472–1492.
[39] M.N. Özişik, H.R.B. Orlande, M.J. Colaço, R.M. Cotta, Finite Difference Methods in Heat Transfer, CRC Press, 2017.

[40] K. Puri, P. Ramachandran, A comparison of SPH schemes for the compressible Euler equations, J. Comput. Phys. (256) (2014) 308–333.
[41] N.J. Quinlan, M. Basa, M. Lastiwka, Truncation error in mesh-free particle methods, Internat. J. Numer. Methods Engrg. 66 (13) (2006) 2064–2085.
[42] P.J. Roache, P.M. Knupp, Completed Richardson extrapolation, Commun. Numer. Methods. Eng. 9 (5) (1993) 365–374.
[43] T. Stranex, S. Wheaton, A new corrective scheme for SPH, Comput. Methods Appl. Mech. Engrg. 200 (2011) 392–402.